

Blue carbon in restored and reference salt marshes in Galveston Bay, Texas



Prepared by:
Anna R. Armitage, Ph.D.
Texas A&M University Galveston Campus
PO Box 1675
Galveston, TX 77553

Prepared for:



TABLE OF CONTENTS

Introduction	1
Methods	2
Field sites	2
Field methods	2
Plant biomass	2
Sediment cores	2
Lab methods.....	5
Plants.....	5
Sediments	5
Radioisotope dating	6
Statistical analyses	6
Results & Analysis	6
Plants.....	6
Biomass	6
Carbon content	6
Sediments	9
Bulk density.....	9
Carbon content	9
Radioisotope dating	12
Summary	15
Acknowledgements.....	17
References	18

LIST OF FIGURES

Figure 1. Area map depicting study sites and approximate time since restoration (in years)..... 4

Figure 2. Core sectioning in the field. 5

Figure 3. Total plant biomass pooled across all species at reference and restored salt marshes in Galveston Bay, Texas. Restored sites were divided into three age categories based on the number of years since planting; site planting dates are provided in Table 1. All restored areas had similar biomass; reference sites had significantly lower biomass than the oldest restored sites. n = 3; error bars represent standard error. 7

Figure 4. Representative photos of a reference site (Sunset Cove) and an old restoration site (Dalehite Cove). Note the plant height relative to the field crew and to the PVC marker poles (arrow indicates 1 m from the sediment surface)..... 7

Figure 5. *Spartina alterniflora* leaf carbon content at reference and restored salt marshes in Galveston Bay, Texas. Restored sites were divided into three age categories based on the number of years since planting; site planting dates are provided in Table 1. n = 3; error bars represent standard error. 8

Figure 6. Sediment bulk density at reference and restored salt marshes in Galveston Bay, Texas. Restored sites were divided into three age categories based on the number of years since planting; site planting dates are provided in Table 1. 10

Figure 7. Sediment carbon content, scaled to megagrams (Mg) per hectare, at reference and restored salt marshes in Galveston Bay, Texas. Restored sites were divided into three age categories based on the number of years since planting; site planting dates are provided in Table 1. n = 3; error bars represent standard error..... 10

Figure 8. Relationship between dry bulk density and sediment percent carbon..... 11

Figure 9. Relationship between percent loss on ignition (LOI) and sediment percent carbon..... 11

Figure 10. Total Pb-210 Activity (disintegrations per minute [DPM]/g Dry Wt.) in sediment core from a young (<10 years old) restored site (Isla del Sol) in Galveston Bay, Texas. 12

Figure 11. Total Pb-210 Activity (disintegrations per minute [DPM]/g Dry Wt.) in sediment core from a restored site between 10-15 years old (Reitan Shelter) in Galveston Bay, Texas. 13

Figure 12. Total Pb-210 Activity (disintegrations per minute [DPM]/g Dry Wt.) in sediment core from an old restored site (> 15 years old; Reitan) in Galveston Bay, Texas. 14

Figure 13. Total Pb-210 Activity (disintegrations per minute [DPM]/g Dry Wt.) in sediment core from a reference site (Christmas Bay) in Galveston Bay, Texas..... 14

LIST OF TABLES

Table 1. List of field sites in Galveston Bay, including coordinates and approximate year planted (for restoration sites). 3

Table 2. Plant biomass and leaf carbon content (as a percent of dry weight) at reference and restored salt marshes in Galveston Bay, Texas; values presented are averages of the three plots sampled at each site..... 8

LIST OF APPENDICES

APPENDIX A. Radioisotope Methods 20

APPENDIX B. Sediment DBD and Total Carbon 22

APPENDIX C. Radioisotope interpretation 25

Introduction

Coastal wetlands provide many ecosystem services, including the sequestration of carbon in vegetation and soil. An essential component of managing these critical services is coastal wetland restoration. The fundamental goal of habitat restoration is to increase the amount of a target habitat and improve the associated ecological functions and services. However, there is an inherent paradox in restoration projects: the act of restoration – site preparation, grading, planting, and initial evaluation – occurs on a relatively short time scale, over a period of a few years. In contrast, the subsequent process of restoration of the ecosystem – including the development of carbon and other nutrient cycles – occurs on time spans often exceeding ten years (Craft et al. 2003, Llewellyn and La Peyre 2011). This basic challenge of restoration – merging near-term actions with long-term measures of success – must be explicitly and quantitatively integrated into coastal management.

Coastal wetlands are important contributors to carbon stocks in marine environments, broadly referred to as blue carbon (Mcleod et al. 2011). Coastal wetlands are unique in their ability to store large quantities of carbon as blue carbon in aboveground biomass, belowground biomass, and soil organic carbon (Mcleod et al. 2011, Adame et al. 2013), but these stocks may be slow to develop following habitat restoration. Carbon can be absorbed from the atmosphere and stored by microbial and plant communities in a process called sequestration. A portion of this carbon is respired by the plants and released back into the atmosphere, but the remainder is converted into biomass that may become sequestered in the soil for decades. The carbon sequestration role of coastal habitats is likely to be of paramount importance in the maintenance of global atmospheric carbon levels, but the burgeoning field of blue carbon still lacks quantitative estimates of carbon storage in many marine habitats. Therefore, the goals of this project were to (1) quantify blue carbon stocks in restored coastal salt marshes in Galveston Bay, Texas, and (2) determine how long it takes for restored marsh blue carbon stocks to approach those in reference wetlands.

Methods

Field sites

Twelve sites around Galveston Bay were identified and classified as reference or restored salt marshes. Restored sites were subdivided into three categories based on time since restoration (Table 1; Figure 1). The restored sites were, according to local knowledge, historical salt marshes that were submerged in the 1960s-1980s due to rapid subsidence in the area (the entire bay experienced rapid subsidence as the oil industry expanded and groundwater was withdrawn at a rapid rate. Groundwater is better managed now and subsidence rates have slowed.). So, to bring the restored sites back up to emergent marsh elevation, dredge material from nearby subtidal areas (possibly from boating channel maintenance) was added to the sites. All restored sites were formed by creating a marsh platform with dredge material followed by planting with *Spartina alterniflora* and other species.

All sites were sampled in Fall 2016; sampling dates fell between September 21 and November 15, 2016. Sampling targeted low elevation marsh zones that were dominated by *Spartina alterniflora*. Three plots were established at each site; plots were spaced at least 50 m apart.

All field and lab methods were based on protocols developed by Conservation International and the International Union for Conservation of Nature (CI/IUCN) (Howard et al. 2014). These methods are comparable to those employed by another regional blue carbon study from Tampa Bay, Florida (Moyer et al. 2016).

Field methods

Plant biomass

Plant biomass was sampled following the protocols for salt marsh grasses developed by CI/IUCN (Howard et al. 2014). At each plot within each site, all of the stems within a representative 10 x 20 cm quadrat were clipped at the sediment surface and pooled into large plastic bags for transport back to the lab.

Sediment cores

Sediment cores were collected following the protocols described by CI/IUCN (Howard et al. 2014). Within each study plot, sediment cores were taken by manually pushing an 87-mm diameter PVC pipe as deep as possible into the ground, typically to a depth of 30-40 cm. Compaction was monitored by measuring the sediment surface inside and outside the core tube. If compaction was greater than 2 cm (~5% of total core length), the core was not used. After the core was inserted into the sediment, a rubber gasket was placed over the top and then the core was dug out of the sediment. Cores were sectioned into 5-cm subsections in the field for bulk density and carbon analyses (Figure 2); core sections were placed in plastic zipper freezer bags for transport to the laboratory at TAMUG, where they were frozen (-20°C) on the day of collection pending future analysis. At a subset of sites (Table 1), an additional core was collected for radioisotope dating analyses; these cores were divided into 2-cm subsections for analysis.

Table 1. List of field sites in Galveston Bay, including coordinates and approximate year planted (for restoration sites).

Site name	Coordinates	Status	Year planted (if applicable)	Age category (years)
Terra Mar ⁺	N 29.135231 W 95.069065	Restored	2010	< 10
Isla del Sol*	N 29.141687 W 95.057532	Restored	2010	< 10
McAllis Point	N 29.177713 W 95.012731	Restored	2011	< 10
Snake Island Cove ⁺	N 29.157969 W 95.028777	Restored	2006	10-15
Reitan shelter*	N 29.324446 W 94.927424	Restored	2002	10-15
Reitan North	N 29.318419 W 94.916602	Restored	2003	10-15
Dalehite	N 29.226260 W 94.943974	Restored	2000	> 15
Reitan**	N 29.315048 W 94.914854	Restored	2000	> 15
Moses Lake	N 29.434187 W 94.947897	Restored	1995	> 15
Sunset Cove ⁺	N 29.150774 W 95.037102	Reference		
Indian Beach	N 29.174242 W 95.008863	Reference		
Christmas Bay*	N 29.048605 W 95.164219	Reference		

* sites where cores were collected for radiocarbon dating analysis

⁺ sites where additional analyses to determine sediment organic content were performed

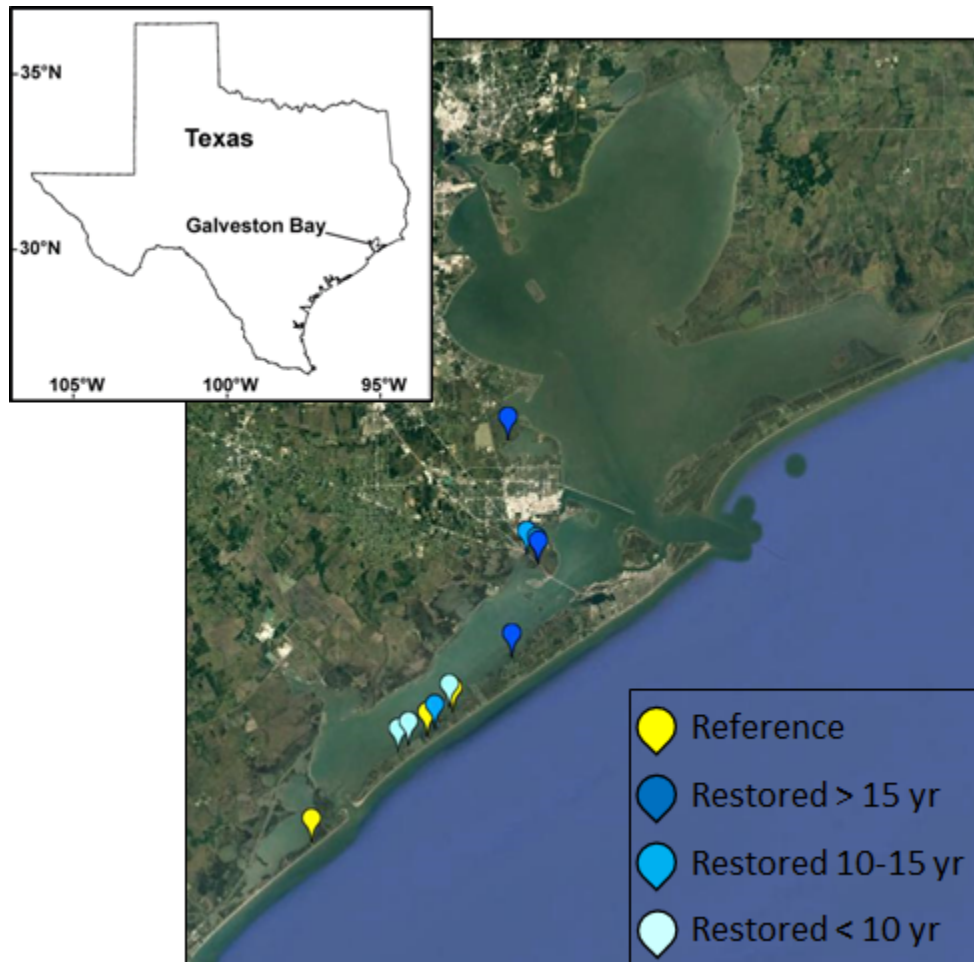


Figure 1. Area map depicting study sites and approximate time since restoration (in years).



Figure 2. Core sectioning in the field.

Lab methods

Plants

Biomass

In the lab we rinsed and dried all aboveground plant tissue and calculated aboveground biomass as dry weight as $\text{g}/0.02\text{m}^2$, which was then converted to a standard reporting unit of kg/m^2 .

Carbon content

Representative dried leaves of *Spartina alterniflora* were ground to a fine powder in a Thomas Wiley® mini-mill. Leaf carbon content was determined using a CHN analyzer (Perkin-Elmer 2400 CHN Analyzer), which reports nutrients as a percent of dry weight.

Sediments

Dry bulk density

Prior to analyses, all 5-cm frozen sediment core sections were freeze dried in the original sample bags for ~1 week until constant weight was achieved. Samples were then weighed and dry bulk density (DBD) was calculated as dry weight (g)/sample volume (cm^3).

Carbon content

After sediment core sections were freeze dried, they were homogenized with a mortar and pestle. Sediment carbon content was determined in the CHN Analyzer as above. For a subset of sites (Table 1), organic content was calculated as the difference in weight before and after loss on ignition (LOI) at 500°C for four hours, and is reported as percent loss (Fourqurean et al. 2012).

Radioisotope dating

A subset of sediment cores were prepared for analysis to estimate soil carbon sequestration rates using Pb-210 (Lead-210) dating at an external lab, Flett Research Ltd. (<http://www.flettresearch.ca/>). These cores were thawed but not dried, double-bagged, and then shipped to Flett Research for complete radioisotope dating analyses. Detailed methods on the dating protocol are provided in Appendix A and can also be accessed at the following link: <http://www.flettresearch.ca/isotopemethods.html>. In brief, Lead-210 (Pb-210) and Cesium-137 (Cs-137) were measured at regular intervals throughout sediment cores to determine the rate of sediment accumulation. Atmospheric depositions of Pb-210 occur at a nearly constant rate, so the accumulation of Pb-210 in the sediment is used to calculate sediment age and accumulation rate. In addition, 2-3 measurements of Radium-226 (Ra-226) were performed in each core to identify the Pb-210 background level (i.e., Pb-210 in excess of the background level indicates atmospheric deposition during sediment accumulation). Radioactive Cs-137 is present in the atmosphere as a result of nuclear testing and releases from reactors; peak emissions occurred in the 1950s and '60s, and accumulation in sediments from the subsequent fallout provides another potential sediment core dating tool.

Statistical analyses

Plant carbon and biomass and soil carbon data were analyzed with 1-way ANOVA, where the dependent variable were the plant and soil biomass, density, or carbon metrics, and the independent variable was site type. Homogeneity of variances was confirmed with a Levene's test of equality of error variances. If there was a significant effect of habitat type, a Tukey HSD post-hoc test was performed to identify homogeneous subset among habitat types. All analyses were performed with SPSS v.24.

Results & Analysis

Plants

Biomass

Spartina alterniflora (smooth cordgrass) dominated all study plots; other occasional species included *Batis maritima* and *Salicornia virginica*.

Total plant biomass was different among site types (ANOVA $df = 3$, $F = 3.875$, $p = 0.056$). Average values for each site are shown in Table 2. Post-hoc tests revealed that all restored sites were statistically similar to each other, but that there was a significant difference between reference and old (> 15 years old) restored sites (Figure 3); reference sites had the lowest plant biomass. A likely explanation for this unexpected result is that the *S. alterniflora* cultivar commonly used in restoration projects around Galveston Bay is derived from the Vermilion strain of this species (collected from Vermilion Bay, Louisiana). This strain often grows to heights exceeding 1.5 meters (Fine and Thomassie 2000), which is taller than local strains (Figure 4). Therefore, the planted variety had correspondingly high biomass, relative to local reference strains.

Carbon content

Carbon content of *Spartina alterniflora* leaf tissue ranged from 36-44 %C. There were no significant differences in leaf carbon content among sites (ANOVA $df = 3$, $F = 0.329$, $p = 0.804$). Average values for each site are shown in Table 2.

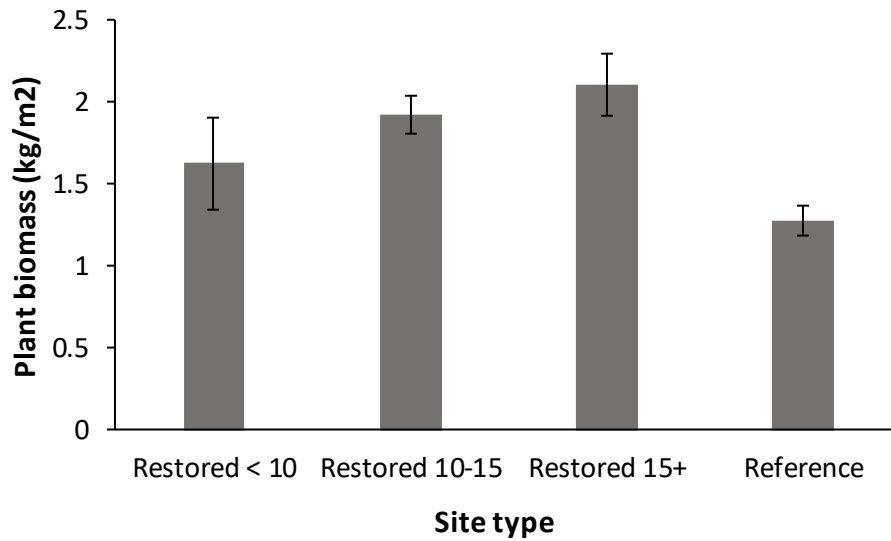


Figure 3. Total plant biomass pooled across all species at reference and restored salt marshes in Galveston Bay, Texas. Restored sites were divided into three age categories based on the number of years since planting; site planting dates are provided in Table 1. All restored areas had similar biomass; reference sites had significantly lower biomass than the oldest restored sites. n = 3; error bars represent standard error.



Figure 4. Representative photos of a reference site (Sunset Cove) and an old restoration site (Dalehite Cove). Note the plant height relative to the field crew and to the PVC marker poles (arrow indicates 1 m from the sediment surface).



Figure 5. *Spartina alterniflora* leaf carbon content at reference and restored salt marshes in Galveston Bay, Texas. Restored sites were divided into three age categories based on the number of years since planting; site planting dates are provided in Table 1. n = 3; error bars represent standard error.

Table 2. Plant biomass and leaf carbon content (as a percent of dry weight) at reference and restored salt marshes in Galveston Bay, Texas; values presented are averages of the three plots sampled at each site.

Site name	Site type	Plant biomass (kg/m ²)	Leaf % carbon
Terra Mar	Restored <10	1.1	44.3
Isla del Sol	Restored <10	1.3	36.2
McAllis Point	Restored <10	1.4	41.0
Snake Island Cove	Restored 10-15	2.0	42.5
Reitan shelter	Restored 10-15	1.1	42.5
Reitan North	Restored 10-15	1.8	42.0
Dalehite	Restored >15	2.1	41.4
Reitan	Restored >15	2.0	43.2
Moses Lake	Restored >15	1.7	41.8
Sunset Cove	Reference	2.0	45.4
Indian Beach	Reference	2.5	43.2
Christmas Bay	Reference	1.8	38.6

Sediments

Bulk density

In general, dry bulk density (DBD) increased with sediment core depth, but patterns were variable among sites (Figure 6). There was no consistent difference in dry bulk density between restored and reference salt marsh sites.

Carbon content

Sediment carbon content, scaled to megagrams (Mg) per hectare, was markedly lower in young restored sites (Figure 7), but there was considerable variability among sites, so this difference was not statistically significant (ANOVA df = 3, F = 1.556, p = 0.274). A complete suite of carbon content metrics is provided in Appendix B.

In cases where direct measurements of sediment carbon content are not logistically or financially feasible, less labor- and cost-intensive approaches may serve as proxies for direct carbon measurements. Specifically, dry bulk density (DBD) and loss on ignition (LOI) are relatively inexpensive, easy measurements, and these metrics may have correlative relationships with sediment %C. These correlations were examined across the study sites in Galveston Bay.

There was a negative exponential relationship between dry bulk density and sediment %C across all sites (Figure 8). The relationship was described by the following equation:

$$(1) \%C = 1.3234e^{-0.277DBD} \quad R^2 = 0.4512$$

The low R^2 value suggests that there was a fair amount of variation in %C that was not explained by DBD. Notably, there were some middle-age restoration sites (10-15 years old) that had very low sediment %C values, and there were some old (<15 years old) that had relatively high sediment %C, suggesting that the variability in sediment sources used to construct the sites reduces the reliability of DBD as a predictor of %C. If restoration sites were excluded from this analysis, and only reference sites were included, a much stronger relationship emerged:

$$(2) \%C = 1.6311e^{-0.432DBD} \quad R^2 = 0.9388$$

Therefore, in Galveston Bay salt marshes, DBD should be used as a predictor of sediment %C only in reference sites.

There was a strong, positive linear relationship between percent loss on ignition (LOI) and sediment %C across all sites (Figure 9). The relationship was described by the following equation:

$$(3) y = 2.7166LOI + 0.3708 \quad R^2 = 0.8645$$

This relationship suggests that LOI may be a more reliable proxy for sediment %C. However, LOI was measured only for a subset of sites and therefore did not capture the range of variability in sediment conditions that is suggested in Figure 6 and Figure 8. Therefore, the use of LOI as a proxy for sediment %C in restored salt marshes in the Galveston Bay region should be used conservatively, and further calibration of the proxy is recommended.

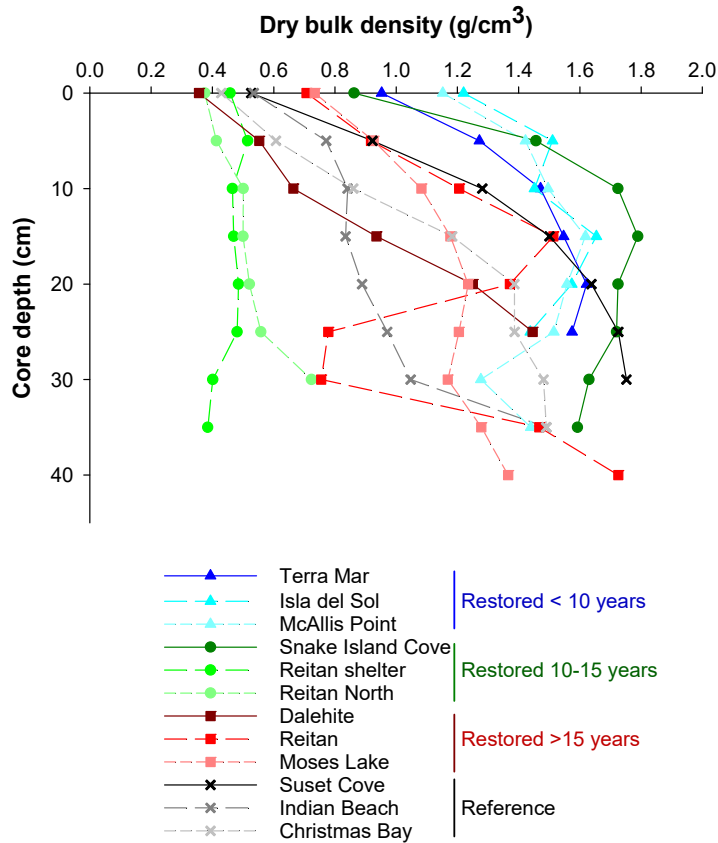


Figure 6. Sediment bulk density at reference and restored salt marshes in Galveston Bay, Texas. Restored sites were divided into three age categories based on the number of years since planting; site planting dates are provided in Table 1.

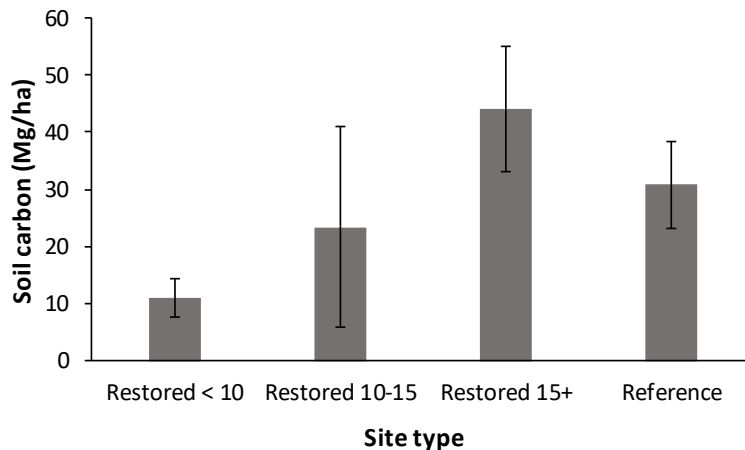


Figure 7. Sediment carbon content, scaled to megagrams (Mg) per hectare, at reference and restored salt marshes in Galveston Bay, Texas. Restored sites were divided into three age categories based on the number of years since planting; site planting dates are provided in Table 1. n = 3; error bars represent standard error

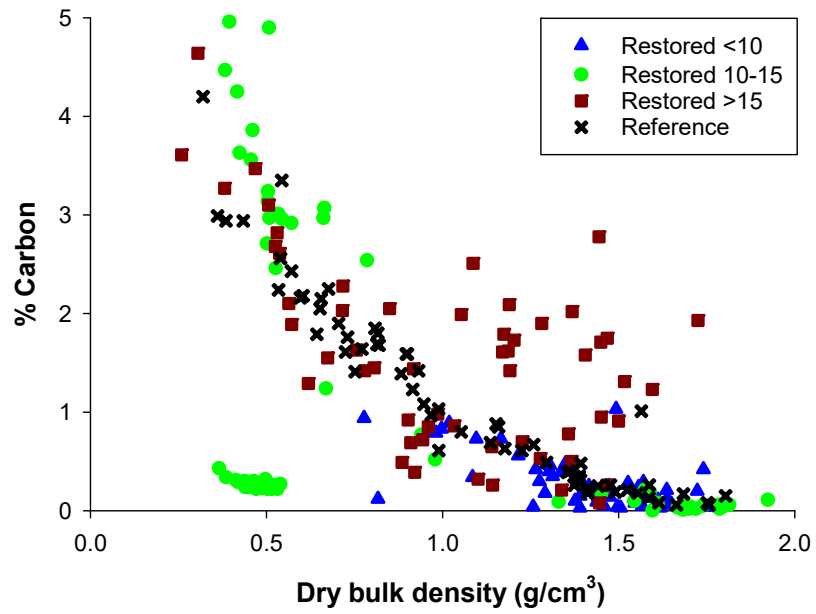


Figure 8. Relationship between dry bulk density and sediment percent carbon.

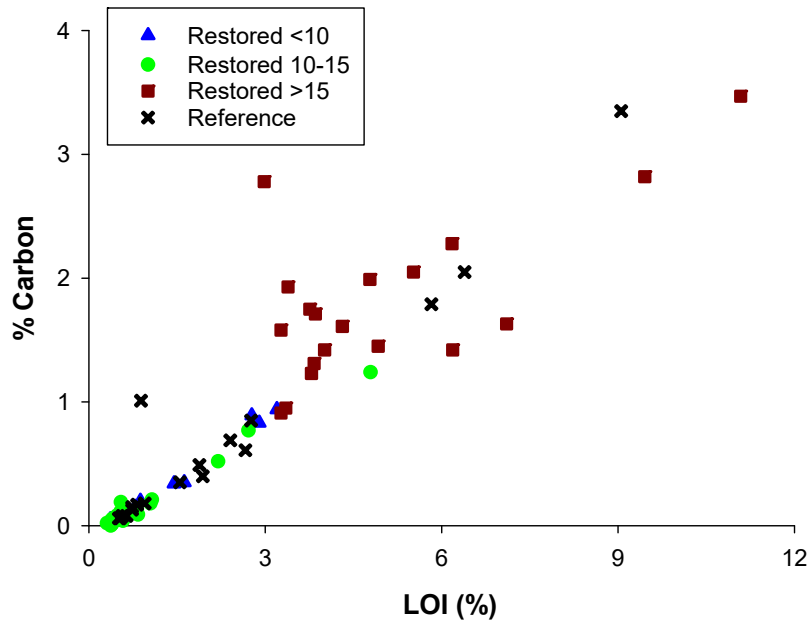


Figure 9. Relationship between percent loss on ignition (LOI) and sediment percent carbon.

Radioisotope dating

The activity of Pb-210, Ra-226 and Cs-137 was determined at two centimeter intervals for four sediment cores, one from each restoration age category and one reference (see Table 1 for sites where radiocarbon dating cores were collected). Detailed interpretations were provided by the analytical contractor (Flett Research, Ltd) and are provided in Appendix C; key results are highlighted below.

Restoration site < 10 years old: Isla del Sol. According to the nearly vertical shape of the Pb-210 profile between 6 - 20 cm (Figure 10), it is likely that soil below 6 cm depth was dredged material placed during site restoration. The approximate site creation date was 2010, suggesting that the top 6 cm of sediment had accumulated since restoration. To estimate soil accumulation rates, a linear regression model of unsupported Pb-210 activity vs. cumulative dry weight (g/cm^2) was applied, where the unsupported Pb-210 activity was calculated by subtracting the nearest neighboring Ra-226 measurement from each total Pb-210 value. The resulting model predicted an average soil accumulation rate of $0.58 \text{ g}/\text{cm}^2/\text{yr}$ ($R^2 = 0.8093$). There was a low but measurable presence of Cs-137 in most sections of this core. The low levels of Cs-137 suggest that (1) the soil accumulation rate since dredge material deposition is high and is diluting Cs-137 activity, AND/OR (2) the absence of fine particulates, to which Cs-137 preferentially adsorbs, makes this sandy soil a poor accumulator of Cs-137. Furthermore, cesium is frequently mobile in organic rich and carbonate sediments, and is less informative on recently deposited sediments (Ritchie and McHenry 1990), so it does not appear to be an effective dating tool in this particular ecosystem.

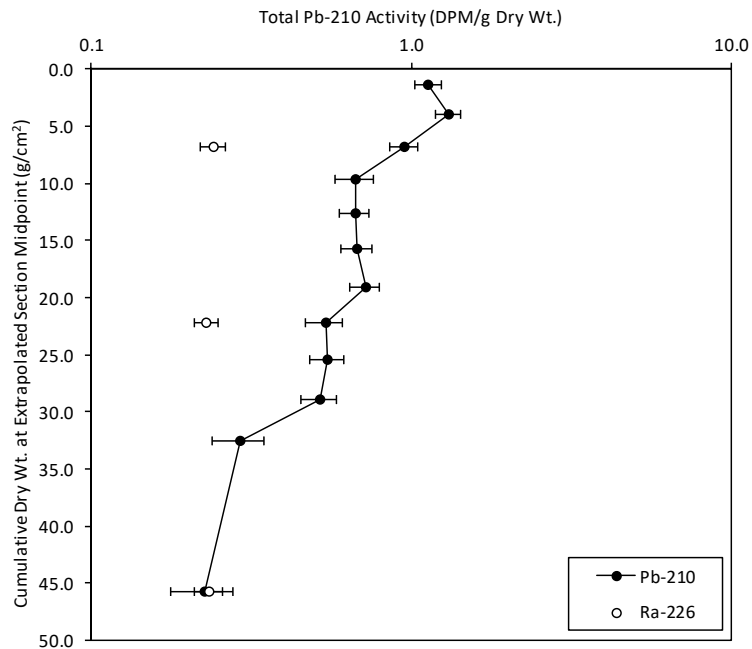


Figure 10. Total Pb-210 Activity (disintegrations per minute [DPM]/g Dry Wt.) in sediment core from a young (<10 years old) restored site (Isla del Sol) in Galveston Bay, Texas.

Restoration site 10-15 years old: Reitan shelter. Activity of Pb-210 was relatively high in this core, and decreased exponentially with depth (Figure 11). The Pb-210 activity (2.65 DPM/g) seen in the bottom section (36 - 38 cm) is significantly higher than the Ra-226 activity measured in the same section, indicating that the background level of Pb-210 has not been achieved in this core. The entire core is likely comprised of material that accumulated since site restoration in 2002. Further, all measurements

of Cs-137 throughout the core were significantly above background levels, indicating that all sections of the core are less than 53 years old (post 1963). The linear regression model was applied as above; the predicted soil accumulation rate was 0.53 g/cm²/yr ($R^2 = 0.9414$).

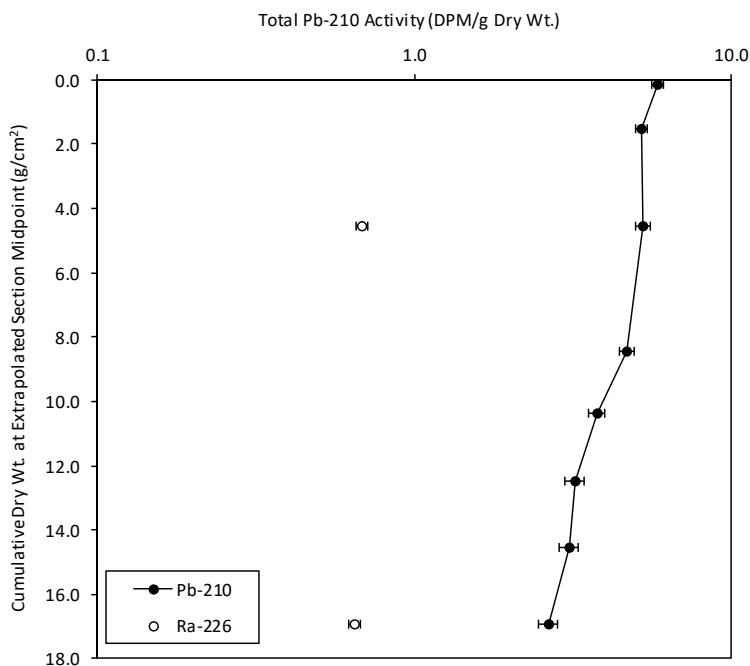


Figure 11. Total Pb-210 Activity (disintegrations per minute [DPM]/g Dry Wt.) in sediment core from a restored site between 10-15 years old (Reitan Shelter) in Galveston Bay, Texas.

Restoration site > 15 years old: Reitan. In this core, detectable atmospheric sourced Pb-210 was observed only in the upper 4 cm (Figure 12). Below 4 cm depth, the sediment was probably dredge material placed during site construction. Since the dredged material does not contain detectable atmospheric sourced Pb-210, it could possibly consist of soil older than 66 years (~ 3 half-lives of Pb-210). Cesium-137 was detected only in the upper 14 cm of the core. The linear regression model could not be applied to this core, because only two samples near the core surface contained detectable unsupported Pb-210, based upon the Ra-226 measurements and the shape of Pb-210 profile. The approximate site creation date was 2000, suggesting that the top 4 cm of sediment had accumulated since restoration. Accordingly, then the average soil accumulation rate at this sampling site was estimated as: 4 cm / 15 years = 0.27 cm/yr, or 4.300 (g/cm²) / 15 years = 0.287 g/cm²/yr.

Reference site: Christmas Bay.

The Pb-210 activity profile of this core showed an irregular, but approximately exponential decrease as a function of depth (Figure 13). The Pb-210 activity (0.58 DPM/g) seen in the bottom section (36 - 38 cm) was significantly higher than the Ra-226 activity measured in the same section, indicating that the background level of Pb-210 had not been achieved in this core. In the upper 13 cm (extrapolated depth), the samples contained a substantial amount of vegetation, while the samples below 16 cm contained primarily clay without any vegetation. The dry bulk density also increased markedly below 16 cm of the core. Even though this site was considered to be a reference marsh, these sediment core observations suggest that the soil below 16 cm depth may have been placed, either through purposeful dredge placement or through a storm sedimentation event. The linear regression model was applied as above; the predicted average soil accumulation rate was 0.1827 g/cm²/yr ($R^2 = 0.7259$). However, there was a

potential sediment slump event (the third and fourth data points from the top in Figure 13). This disturbance in the sediment accumulation process increases the uncertainty in modeling results. All measurements of Cs-137 throughout the core were significantly above background levels, indicating that all sections of the core are less than 53 years old (post 1963).

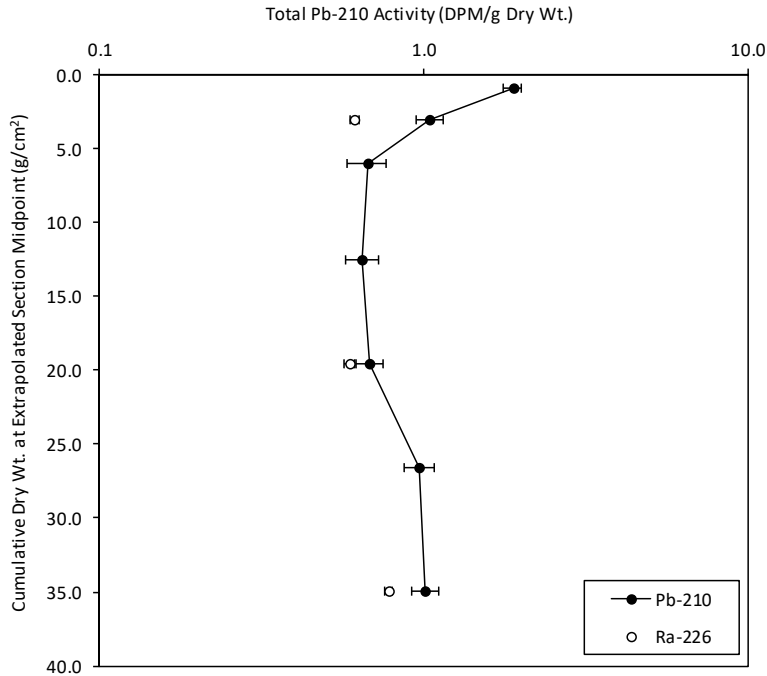


Figure 12. Total Pb-210 Activity (disintegrations per minute [DPM]/g Dry Wt.) in sediment core from an old restored site (> 15 years old; Reitan) in Galveston Bay, Texas.

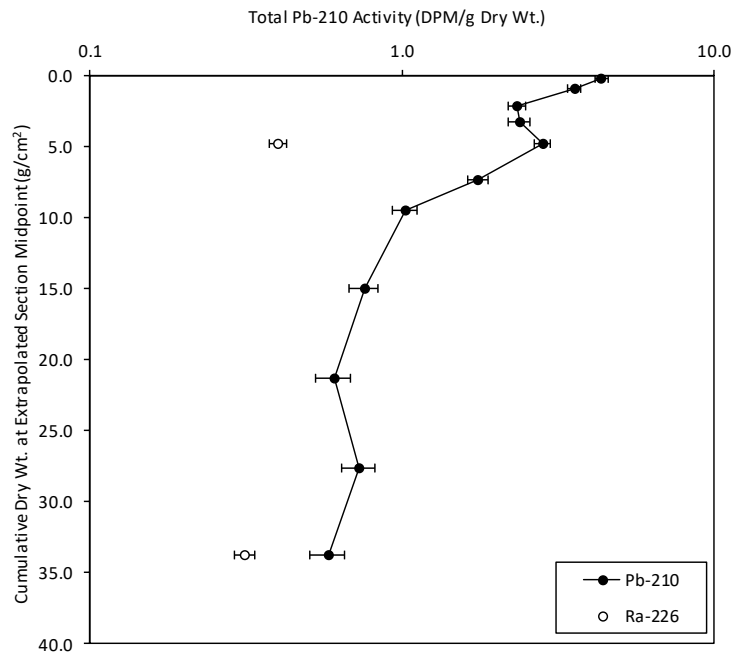


Figure 13. Total Pb-210 Activity (disintegrations per minute [DPM]/g Dry Wt.) in sediment core from a reference site (Christmas Bay) in Galveston Bay, Texas.

Summary

Plant carbon stocks quickly recovered in restored sites, in most cases exceeding reference site values within five years. The rapid establishment of emergent plants is a relative common occurrence in Gulf Coast wetland restoration projects (Webb and Newling 1985, Edwards and Mills 2005, Armitage et al. 2014). This rapid recovery may have also been a function of the reported use of a particularly fast-growing, tall strain of *S. alterniflora* in restored sites. There are few studies that have produced directly comparable values of emergent plant carbon stock in restored Gulf of Mexico salt marshes, but those that do exist are similar ($\sim 1\text{-}3 \text{ kg m}^{-2}$) to the values in the current study (Madrid et al. 2012, Moyer et al. 2016; converted from megagrams/hectare). Furthermore, plant carbon stock is likely correlated to productivity, and productivity in Texas marshes is comparable to other regions of the Gulf (Mendelssohn and Morris 2002).

The size of the plant carbon stock is directly and positively correlated with the area planted (Madrid et al. 2012). Accordingly, plant carbon stocks should be higher in areas with a relatively high ratio of area of emergent: aquatic habitat. Therefore, if the primary objective of a restoration project is to augment carbon stock, then emergent habitat should be prioritized over subtidal or aquatic habitat. However, if that strategy is pursued, then it must be conceded that ecosystem functions associated with tidal flats and subtidal habitats might be compromised (e.g., fishery habitat; Rozas et al. 2005).

Although the plant carbon stock often develops quickly in restored sites, it typically isn't a primary goal of blue carbon mitigation projects, since soil carbon stocks are more recalcitrant on decadal scales and beyond (Connor et al. 2001, Duarte et al. 2013). In our project, soil carbon stocks (30-50 Mg/ha) approached reference conditions in sites that were more than 15 years old, but stocks were variable across sites, regardless of restoration status; some restoration sites exceeded reference values, and others did not. Soil carbon stocks in Texas reference sites were comparable to those in restored and reference salt marshes in Tampa, Florida (Moyer et al. 2016), but were well below global averages (162 Mg/ha; Duarte et al. 2013), though it should be noted that salt marsh soil carbon stocks vary widely across the globe. Our study also demonstrated that there is substantial variation among study sites within a region in both carbon stocks and accumulation rates (as measured with radioisotope dating). Ultimately, this body of work illustrates that carbon stocks are spatially heterogeneous and that high resolution, site-level studies are needed to inform regional-level policies and blue carbon mitigation strategies.

These results demonstrate that salt marsh restoration can augment the redevelopment of blue carbon stocks at a site-level scale. However, restoration projects are relatively small in area and only partly compensate for regional habitat loss due to subsidence, development, and other impacts. The potential for habitat restoration to recreate blue carbon stocks is further complicated by ongoing landscape-level shifts in coastal wetland plant communities in Texas, where black mangroves (*Avicennia germinans*) are becoming more common (Armitage et al. 2015). Currently, the coast-level areal extent of mangroves is relatively small and makes a minor contribution to blue carbon stocks in Texas, but ongoing changes in plant distribution and shifting restoration strategies may further alter regional blue carbon storage potential.

Regional and site-specific data are essential to parameterize the emerging blue carbon market (Sutton-Grier and Moore 2016). Given that Galveston Bay soil carbon stocks are relatively modest, blue carbon may not stand alone as a primary market driver for local wetland restoration. However, there are many other incentives to restore coastal wetlands in Galveston Bay and throughout the Gulf of Mexico,

including fishery support (Rozas et al. 2005), shoreline stabilization (Peterson et al. 2008), and ecotourism (Needles et al. 2015). Therefore, the blue carbon value of plants and soils in Galveston Bay wetlands is an added benefit that will increase the suite of ecosystem benefits provided by coastal wetland restoration.

Acknowledgements

Many thanks are extended to the dedicated crew that conducted field sampling and laboratory analyses, especially Kathleen Bowers, Scott Hall, Jake Sigren, Rebekkah Bergren, Rachael Glazner, and Monika McGuinness. Accenture and Restore America's Estuaries graciously provided funding and logistical support for this project. Thank you to the Galveston Bay Foundation for site access permissions and guidance in the design of this project.

References

- Adame, M. F., J. B. Kauffman, I. Medina, J. N. Gamboa, O. Torres, J. P. Caamal, M. Reza, and J. A. Herrera-Silveira. 2013. Carbon Stocks of Tropical Coastal Wetlands within the Karstic Landscape of the Mexican Caribbean. *PLoS ONE* **8**:e56569.
- Armitage, A. R., W. E. Highfield, S. D. Brody, and P. Louchouart. 2015. The contribution of mangrove expansion to salt marsh loss on the Texas gulf coast. *Plos One* **10**:e0125404.
- Armitage, A. R., C.-K. Ho, E. N. Madrid, M. T. Bell, and A. Quigg. 2014. The influence of habitat construction technique on the ecological characteristics of a restored brackish marsh. *Ecological Engineering* **62**:33-42.
- Connor, R. F., G. L. Chmura, and C. B. Beecher. 2001. Carbon accumulation in Bay of Fundy salt marshes: implications for restoration of reclaimed marshes. *Global Biogeochemical Cycles* **15**:943-954.
- Craft, C., P. Megonigal, S. Broome, J. Stevenson, R. Freese, J. Cornell, L. Zheng, and J. Sacco. 2003. The pace of ecosystem development of constructed *Spartina alterniflora* marshes. *Ecological Applications* **13**:1417-1432.
- Duarte, C. M., I. J. Losada, I. E. Hendriks, I. Mazarrasa, and N. Marbà. 2013. The role of coastal plant communities for climate change mitigation and adaptation. *Nature Climate Change* **3**:961-968.
- Edwards, K. R., and K. P. Mills. 2005. Aboveground and belowground productivity of *Spartina alterniflora* (smooth cordgrass) in natural and created Louisiana salt marshes. *Estuaries* **28**:252-265.
- Fine, G., and G. Thomassie. 2000. Release Brochure Vermilion Smooth Cordgrass (*Spartina alterniflora*). 5830, Galliano, LA.
- Fourqurean, J. W., G. A. Kendrick, L. S. Collins, R. M. Chambers, and M. A. Vanderklift. 2012. Carbon, nitrogen and phosphorus storage in subtropical seagrass meadows: examples from Florida Bay and Shark Bay. *Marine and Freshwater Research* **63**:967-983.
- Howard, J., S. Hoyt, K. Isensee, E. Pidgeon, and M. Telszewski, editors. 2014. Coastal Blue Carbon: Methods for assessing carbon stocks and emissions factors in mangroves, tidal salt marshes, and seagrass meadows. Conservation International, Intergovernmental Oceanographic Commission of UNESCO, International Union for Conservation of Nature, Arlington, Virginia, USA.
- Llewellyn, C., and M. La Peyre. 2011. Evaluating ecological equivalence of created marshes: comparing structural indicators with stable isotope indicators of blue crab trophic support. *Estuaries and Coasts* **34**:172-184.
- Madrid, E. N., A. Quigg, and A. R. Armitage. 2012. Marsh construction techniques influence net plant carbon capture by emergent and submerged vegetation in a brackish marsh in the northwestern Gulf of Mexico. *Ecological Engineering* **42**:54-63.
- Mcleod, E., G. L. Chmura, S. Bouillon, R. Salm, M. Björk, C. M. Duarte, C. E. Lovelock, W. H. Schlesinger, and B. R. Silliman. 2011. A blueprint for blue carbon: toward an improved understanding of the role of vegetated coastal habitats in sequestering CO₂. *Frontiers in Ecology and the Environment* **9**:552-560.
- Mendelssohn, I. A., and J. T. Morris. 2002. Eco-physiological controls on the productivity of *Spartina alterniflora* Loisel. Pages 59-80 in M. P. Weinstein and D. A. Kreeger, editors. Concepts and controversies in tidal marsh ecology. Kluwer Academic Publishers, Dordrecht.
- Moyer, R. P., K. R. Radabaugh, C. E. Powell, I. Bociu, A. R. Chappel, B. C. Clark, S. Crooks, and S. Emmett-Mattox. 2016. Quantifying carbon stocks for natural and restored mangroves, salt marshes and salt barrens in Tampa Bay. Restore America's Estuaries, USA.

- Needles, L. A., S. E. Lester, R. Ambrose, A. Andren, M. Beyeler, M. S. Connor, J. E. Eckman, B. A. Costa-Pierce, S. D. Gaines, and K. D. Lafferty. 2015. Managing bay and estuarine ecosystems for multiple services. *Estuaries and Coasts* **38**:35-48.
- Peterson, C. H., K. W. Able, C. F. DeJong, M. F. Piehler, C. A. Simenstad, and J. B. Zedler. 2008. Practical proxies for tidal marsh ecosystem services: application to injury and restoration. Pages 221-266 *in* D. W. Sims, editor. *Advances in Marine Biology*, Vol 54.
- Ritchie, J. C., and J. R. McHenry. 1990. Application of radioactive fallout cesium-137 for measuring soil erosion and sediment accumulation rates and patterns: a review. *Journal of Environmental Quality* **19**:215-233.
- Rozas, L. P., P. Caldwell, and T. J. Minello. 2005. The fishery value of salt marsh restoration projects. *Journal of Coastal Research* **SI 40**:37-50.
- Sutton-Grier, A. E., and A. Moore. 2016. Leveraging carbon services of coastal ecosystems for habitat protection and restoration. *Coastal Management*:259-277.
- Webb, J. W., and C. J. Newling. 1985. Comparison of natural and man-made salt marshes in Galveston Bay complex, Texas. *Wetlands* **4**:75-86.

APPENDIX A. RADIOISOTOPE METHODS

6/28/2017

Radioisotope Methods at Flett Research Ltd.

Home

Mercury

Radioisotope

Personnel

Pricing

Contact Us

Site Map

>>FLETT HOME PAGE >> RADIOISOTOPES >> METHODS & RESOURCES

Flett Research - Radioisotope Methods

Cesium-137 (Cs-137) in sediment and soil is determined by counting the gamma emissions at 661.6 KeV that are emitted in 82.5% of the decays. The gamma radiation is relatively strong and therefore penetrates through several centimetres of sediment material with little attenuation. This procedure is modified from EML HASL-300 Method Ga-01-R. The method detection limit (MDL) with our HPGe detector is 0.3 DPM/g (95% confidence) for an 80,000 second counting period when measuring 9 g of dry sample. The method detection limit can be decreased to 0.1 DPM/g if 32 g of sample is used.

Lead-210 (Pb-210) in sediment, soil and peat is by measurement of the Po-210 grand daughter which is in secular equilibrium with Pb-210 within 2 years of Pb-210 deposition. This procedure is modified from Eakins and Morrison (1978). Samples are first spiked with a Po-209 yield tracer, then digested in hot nitric acid. The digest is dried and made up in 1.5 N HCl and then the Po-210 and Po-209 alpha emitting isotopes are plated out on silver planchets followed by alpha spectrometry to determine the activity of the polonium isotopes. In the case of sediment and soil samples, an initial cleanup of samples may be done by distilling the polonium out of the samples at 500°C prior to nitric acid digestion. The detection limit (MDL) for 0.25 - 0.5 g (dry wt.) sample is between 0.1 - 0.2 DPM Po-210/g dry sample at a 95% confidence level for 60,000 second counting time. This can vary slightly and depends upon the amount of sample and the detector and recovery efficiency of each sample.

Radium-226 (Ra-226) in sediment, soil and peat is determined by radon-222 emanation. This procedure is modified from that of Mathieu *et al.* (1988). The method detection limit (MDL) is dependant on the amount of sample analyzed. For a 60,000 second counting time the MDL @ 95% confidence for 2g of dry samples is 0.1 DPM/g and for 0.5g of dry samples is 0.5 DPM/g.

Methods References:

Environmental Measurements Laboratory, US Department of Energy - HASL-300 Method Ga-01-R Gamma Emitters in the Environment by Energy, HASL EML Procedures Manual, 28th Edition, February 1997.

Eakins, J. D. and R. T. Morrison. 1978. A new procedure for the determination of lead-210 in lake and marine sediments. *International Journal of Applied Radiation and Isotopes*. 29, 531-536.

Mathieu, G.G., P.E. Biscaye, R.A. Lupton and D.E. Hammond. System for measurement of ²²²Rn at low levels in natural waters. 1988. *Health Physics*. 55, 989 – 992.

Other References:

Appleby, P.G. and F. Oldfield. 1978. The calculation of Lead-210 dates assuming a constant rate of supply of unsupported Pb-210 to the sediment. *Catena*. 5, 1-8.

Flynn, W.W. 1968. The determination of low levels of Polonium-210 in environmental materials. *Anal. Chim. Acta*. 43, 221-227.

- Ritchie, J.C. and J. R. McHenry. 1990. Application of radioactive fallout cesium-137 for measuring soil erosion and sediment accumulation rates and patterns: a review. *J. Environ. Qual.* 19, 215-233.
- Carter, M.W. and A.A. Moghissi. 1977. Three decades of nuclear testing. *Health Phys.* 33(1), 55-71.
- Pennington, W., R.S. Cambray and E.M. Fisher. 1973. Observations on lake sediments using fallout Cs-137 as a tracer. *Reprint from Nature.* 242(5396), 324-326. March 30, 1973.
- Durham, R.W. and S.R. Joshi. 1980. The Pb-210 and Cs-137 profiles in sediment cores from Lakes Matagami and Quevillon, northwest Quebec, Canada. *CAN. J. Earth Sci.* 17, 1746-1750.
- Pourchet, M. and J.F. Pinglot. 1989. Cesium-137 and Lead-210 in Alpine lake sediments: measurements and modelling of mixing processes. *Journal of Geophysical Research.* 94(C9), 12,761-12,770. September 15, 1989.
- Marine Radioecology, Final report of the Nordic Nuclear Safety Research Project EKO-1, June 1998.
- Snidvongs, A., G.M. McMurtry and S.V. Smith. 1992. Pb-210 and Cs-137 in sediments and soils of Tomales Bay Watershed, Northern California. Department of Oceanography, Univ. of Hawaii at Manoa Honolulu, HI 96822, U.S.A. Aug 1992.
- Anderson, R.F., S.L. Schiff and R.H. Hesslein. 1987. Determining sediment accumulation and mixing rates using Pb-210, Cs-137, and other tracers: Problems due to postdepositional mobility or coring artifacts. *Canadian Journal of Fisheries and Aquatic Sciences.* 44(S1), 231-250.
- Friedlander, Kennedy and Miller. 1964. Nuclear and Radiochemistry-2nd Edition.
- Mathieu, G.G. Appendix I - Rn²²²-Ra²²⁶ Technique of Analyses. 1977. Transport and transfer rates in the waters of the continental shelf. Contract EY 76-S-02-2185.

For additional information, contact Dr. Robert Flett at flett@flettresearch.ca

Return to the [Flett Research Radioisotope Page.](#)

[return to the top](#)

Flett Research Ltd - 440 DeSalaberry Ave - Winnipeg Manitoba CANADA R2L 0Y7
Phone/Fax: (204) 667-2505

APPENDIX B. SEDIMENT DBD AND TOTAL CARBON

Sediment dry bulk density and total carbon composition in reference and restored salt marsh sites. Values reported are averages of depth intervals of n plots (up to 3 plots per depth interval); scaled carbon stock values are for whole cores.

Site name	Site type	Depth (cm)	Dry bulk density (g/cm ³)	Total % carbon	Carbon density (g/cm ³)	n	Scaled carbon stock (MgC/ha)
Terra Mar	Restored <10	0-5	0.95	0.70	1.91	3	7.61
		5-10	1.27	0.48	1.65	3	
		10-15	1.47	0.10	0.44	3	
		15-20	1.55	0.05	0.21	3	
		20-25	1.62	0.03	0.16	3	
		25-30	1.57	0.03	0.15	3	
		Isla del Sol	Restored <10	0-5	1.22	0.59	
5-10	1.51			0.22	0.97	3	
10-15	1.45			0.14	0.61	3	
15-20	1.65			0.07	0.34	3	
20-25	1.57			0.06	0.31	3	
25-30	1.44			0.09	0.38	1	
McAllis Point	Restored <10			0-5	1.15	0.32	1.21
		5-10	1.42	0.30	1.25	3	
		10-15	1.50	0.21	0.92	3	
		15-20	1.62	0.14	0.67	3	
		20-25	1.56	0.18	0.84	3	
		25-30	1.52	0.42	1.76	3	
		30-35	1.28	0.40	1.37	3	
		35-40	1.44	0.56	2.43	3	
Snake Island Cove	Restored 10-15	0-5	0.86	0.84	2.04	3	7.30
		5-10	1.46	0.15	0.68	3	
		10-15	1.72	0.08	0.43	3	
		15-20	1.79	0.04	0.21	3	
		20-25	1.72	0.05	0.24	3	
		25-30	1.72	0.03	0.15	3	
		30-35	1.63	0.03	0.13	3	
		35-40	1.59	0.15	0.68	2	
Reitan shelter	Restored 10-15	0-5	0.46	0.31	0.42	3	4.34
		5-10	0.52	0.27	0.41	3	
		10-15	0.47	0.24	0.34	3	
		15-20	0.47	0.23	0.33	3	
		20-25	0.49	0.23	0.33	3	
		25-30	0.48	0.25	0.35	3	
		30-35	0.40	0.37	0.43	2	
		35-40	0.38	0.34	0.39	1	

Site name	Site type	Depth (cm)	Dry bulk density (g/cm ³)	Total % carbon	Carbon density (g/cm ³)	n	Scaled carbon stock (MgC/ha)
Reitan North	Restored 10-15	0-5	0.38	4.91	5.41	3	58.49
		5-10	0.41	4.68	5.70	3	
		10-15	0.50	3.17	4.67	3	
		15-20	0.50	3.08	4.54	3	
		20-25	0.52	2.87	4.44	3	
		25-30	0.56	3.74	6.10	3	
		30-35	0.72	2.76	5.89	2	
Dalehite	Restored >15	0-5	0.36	3.78	3.88	3	24.10
		5-10	0.55	2.47	3.84	3	
		10-15	0.66	1.66	2.89	3	
		15-20	0.94	1.20	2.34	3	
		20-25	1.25	0.56	1.89	2	
		25-30	1.45	0.08	0.34	1	
Reitan	Restored >15	0-5	0.71	2.32	4.49	3	61.62
		5-10	0.92	2.14	5.42	3	
		10-15	1.21	1.65	5.44	3	
		15-20	1.51	1.64	7.27	3	
		20-25	1.37	1.44	5.85	3	
		25-30	0.78	1.42	3.28	1	
		30-35	0.75	1.63	3.66	1	
		35-40	1.47	1.75	7.64	1	
Moses Lake	Restored >15	0-5	0.73	1.18	2.45	3	46.58
		5-10	0.93	1.07	2.94	3	
		10-15	1.08	1.76	5.74	3	
		15-20	1.18	1.33	4.70	3	
		20-25	1.23	1.17	4.63	2	
		25-30	1.20	1.42	5.17	3	
		30-35	1.17	0.62	2.26	3	
		35-40	1.28	0.53	2.01	1	
		40-45	1.37	0.50	2.03	1	
Sunset Cove	Reference	0-5	0.53	2.78	4.25	3	19.26
		5-10	0.92	1.03	2.51	3	
		10-15	1.28	0.56	2.09	3	
		15-20	1.50	0.24	1.02	3	
		20-25	1.64	0.41	1.95	3	
		25-30	1.73	0.10	0.50	3	
		30-35	1.75	0.08	0.42	1	

Site name	Site type	Depth (cm)	Dry bulk density (g/cm ³)	Total % carbon	Carbon density (g/cm ³)	n	Scaled carbon stock (MgC/ha)
Indian Beach	Reference	0-5	0.53	2.48	3.76	3	45.03
		5-10	0.77	1.64	3.77	3	
		10-15	0.84	1.75	4.35	3	
		15-20	0.83	1.75	4.23	3	
		20-25	0.89	1.32	3.32	3	
		25-30	0.97	1.22	3.38	3	
		30-35	1.05	0.96	2.88	3	
		35-40	1.49	0.37	1.61	2	
Christmas Bay	Reference	0-5	0.43	3.13	3.78	3	28.19
		5-10	0.61	2.25	4.04	3	
		10-15	0.86	1.40	3.09	3	
		15-20	1.18	0.65	2.15	3	
		20-25	1.39	0.29	1.20	3	
		25-30	1.39	0.28	1.15	3	
		30-35	1.48	0.24	1.05	3	
		35-40	1.49	0.19	0.84	1	

APPENDIX C. RADIOISOTOPE INTERPRETATION

Radioisotope dating interpretation and data provided by Flett Research, Ltd.

RESTORATION SITE <10 YEARS OLD: ISLA DEL SOL

INTERPRETATION

Observations:

The Pb-210 activity profile of this core shows an irregular, but approximately exponential decrease as a function of depth. The maximum activity of 1.31 DPM/g observed in section 2 (depth 2 - 4 cm) is about 6 times the lowest activity of 0.23 DPM/g in the bottom section (extrapolated depth 25 - 30 cm). The Pb-210 activity in the surface section (depth 0 - 2 cm) is lower than the adjacent section (depth 2 - 4 cm), and this probably represents increasing soil accumulation rates, and/or physical mixing, and/or diffusion of Pb-210 across a redox gradient, and/or incomplete diagenesis of surface soil, and/or incomplete ingrowth of the Po-210 granddaughter actually being measured.

The dry bulk density in this core generally increases from 1.300 g/cm³ in the uppermost section to 1.886 g/cm³ in section 11 (extrapolated depth 10 - 25 cm), and then drops to 1.420 g/cm³ in the bottom section.

Ra-226 was measured at 0.24, 0.23 and 0.23 DPM/g in sections 4 - 6 cm, 14 - 16 cm and 28 - 30 cm respectively. Net unsupported Pb-210 was calculated by subtracting the nearest neighbouring Ra-226 measurement from each total Pb-210 value. The Pb-210 activity (0.23 DPM/g) seen in the bottom section (depth 28 - 30 cm) is identical to the Ra-226 activity measured in the same section, indicating that the background level of Pb-210 has been achieved in this core.

Cs-137 was measured in all 8 sections in the upper 16 cm of the core. The Cs-137 activities were very low with no detectable Cs-137 observed in this core interval.

Since the salinity was not measured in situ, it is estimated as 17.5 g/kg, the average of 10 g/kg and 25 g/kg (a range suggested by client). All Pb-210, Ra-226 and Cs-137 activities within this written report have been salt corrected.

Regression model of Unsupported Pb-210 activity vs. Cumulative Dry Weight (g/cm²):

When applying the linear regression model, it is assumed that the input of Pb-210 and the soil accumulation rate are constant. Although variation in the soil accumulation rate is apparent, the linear regression model was applied to sections 1 - 10 (depth 0 - 20 cm), because it appears that the average soil accumulation rate in this core interval will be reasonably estimated. This estimate of soil accumulation rate is used to calibrate the CRS model.

The regression model predicts ($R^2 = 0.8093$) an average soil accumulation rate of 0.5799 g/cm²/yr when the unsupported Pb-210 activity was calculated by subtracting the nearest neighbouring Ra-226 measurement from each total Pb-210 value. The age at the bottom of any core section can be estimated by dividing the cumulative dry weight/cm² by the accumulation rate. For example, the age at the bottom of section 5 (depth 10 cm) is calculated as $14.001 / 0.5799 = 24.1$ yr.

CRS model of Age at bottom of Extrapolated section in years vs. Depth of bottom edge of current section in cm:

The CRS model assumes constant input of Pb-210 and a core that is long enough to include all of the measurable atmospheric source Pb-210, i.e. it contains a complete Pb-210 inventory. Due to the sudden decrease in Pb-210 activity in the 20 - 22 cm section, it is suspected that this core is truncated, i.e. less than ~60 years of modern soil is overlying an older basement soil. This leads to the conclusion that the Pb-210 inventory is incomplete and therefore the CRS model cannot be applied in the normal way.

However, in this core it is possible to calibrate the CRS model against the linear regression model, and therefore allow the CRS model to be used. The total atmospheric Pb-210 inventory (DPM/cm²), required in the CRS model calculation, has been chosen (19.781 DPM/cm²) such that the CRS model predicted exactly the same average soil accumulation rate (0.5799 g/cm²/yr) as the linear regression model in the core interval of 0 - 20 cm. With the CRS model calibrated, it has been used to calculate ages for the upper 20 cm of the core.

The average soil accumulation rate, from core surface to the extrapolated bottom depth of any section, can be calculated by dividing the cumulative dry mass at the bottom of the extrapolated section by the calculated age at that depth. For example, the average soil accumulation rate, from the core surface to the bottom of section 5 (depth 10 cm) can be calculated as: $14.001 / 21.9 = 0.6393 \text{ g/cm}^2/\text{yr}$.

Conclusion:

The lack of detectable Cs-137 suggests that (1) the soil accumulation rate is so high that the Cs-137 is diluted out to undetectability AND/OR (2) the absence of fine particulates, to which Cs-137 preferentially adsorbs, makes this sandy soil a poor accumulator of Cs-137. The low activity of excess (i.e. atmospheric sourced) Pb-210 can also be attributed to the same factors.

Over the core interval of 0 - 20 cm, the average soil accumulation rate estimated by the CRS model has been forced to exactly coincide with the linear regression estimate of 0.5799 g/cm²/yr. Although the CRS calculated ages depend upon the results of the linear regression model, the CRS model is to be preferred because it should provide accurate age predictions at the bottom of each section even though the soil accumulation rate is changing with time.

Overall, the analytical quality of radioisotope data (based upon the results of repeat analyses and blanks) is considered good.

Alternative interpretation:

The above interpretation is based upon the assumption that it is a non-disturbed core, i.e. the soil accumulated regularly at this sampling site. However, according to the background information of this project and the nearly vertical shape of Pb-210 profile in core interval of 6 - 20 cm, it is possible that soil below 6 cm depth was due to dredged material placement.

Section 3 (depth 4 - 6 cm) appears to be a mix of dredge material and regularly accumulated soil. If one assumes that 1) dredged material placement occurred 15 years ago, and 2) at 5 cm depth (midpoint depth of section 4 - 6 cm) it represents the surface of dredged material, i.e. natural accumulation of soil started at 5 cm, then the average soil accumulation rate at this sampling site can be estimated as: $5 \text{ cm} / 15 \text{ years} = 0.33 \text{ cm/yr}$, or $6.750 \text{ (g/cm}^2) / 15 \text{ years} = 0.45 \text{ g/cm}^2/\text{yr}$.

RESTORATION SITE 10-15 YEARS OLD: REITAN SHELTER

INTERPRETATION

Observations:

The Pb-210 activity profile of this core shows an irregular, but approximately exponential decrease as a function of depth. The maximum activity of 5.86 DPM/g observed in the uppermost section (extrapolated depth 0 - 3 cm) is about 2 times the lowest activity of 2.65 DPM/g in the bottom section (extrapolated depth 34 - 38 cm). The dry bulk density in this core increases from 0.166 g/cm³ in the uppermost section to 0.509 g/cm³ in section 3 (extrapolated depth 3 - 8 cm), varies between 0.479 - 0.540 g/cm³ in core interval of 3 - 34 cm (extrapolated depth) and then drops to 0.312 g/cm³ in the bottom section.

Ra-226 was measured at 0.68 and 0.65 DPM/g in the 10 - 12 cm section and the 36 - 38 cm section, respectively. Net unsupported Pb-210 was calculated by subtracting the nearest neighbouring Ra-226 measurement from each total Pb-210 value. The Pb-210 activity (2.65 DPM/g) seen in the bottom section (36 - 38 cm) is significantly higher than the Ra-226 activity measured in the same section, indicating that the background level of Pb-210 has not been achieved in this core.

Cs-137 was measured in 12 sections throughout the entire core. All the Cs-137 activities were significantly above background. In the upper 28 cm of the core, the Cs-137 activities vary between 0.35 - 0.62 DPM/g. Below 28 cm depth, the Cs-137 activities gradually increase to 2.02 DPM/g in section 34 - 36 cm and then slightly drop to 1.67 DPM/g in the bottom section (36 - 38 cm).

Since the salinity was not measured in situ, it is estimated as 17.5 g/kg, the average of 10 g/kg and 25 g/kg (a range suggested by client). All Pb-210, Ra-226 and Cs-137 activities within this written report have been salt corrected.

Regression model of Unsupported Pb-210 activity vs. Cumulative Dry Weight (g/cm²):

When applying the linear regression model, it is assumed that the input of Pb-210 and the soil accumulation rate are constant. Although variation in the soil accumulation rate is apparent, the linear regression model was applied to the entire core (0 - 38 cm), because it appears that the average soil accumulation rate will be reasonably estimated. This estimate of soil accumulation rate is used to calibrate the CRS model.

The regression model predicts ($R^2 = 0.9414$) an average soil accumulation rate of 0.5262 g/cm²/yr when the unsupported Pb-210 activity was calculated by subtracting the nearest neighbouring Ra-226 measurement from each total Pb-210 value. The age at the bottom of any core section can be estimated by dividing the cumulative dry weight/cm² by the accumulation rate. For example, the age at the bottom of section 12 (extrapolated depth 25 cm) is calculated as $11.390 / 0.5262 = 21.6$ yr.

CRS model of Age at bottom of Extrapolated section in years vs. Depth of bottom edge of current section in cm:

The CRS model assumes constant input of Pb-210 and a core that is long enough to include all of the measurable atmospheric source Pb-210, i.e. it contains a complete Pb-210 inventory. Since the second assumption is not satisfied in this core (background has not been achieved), it is not normally possible to apply the CRS model.

However, in this core it is possible to calibrate the CRS model against the linear regression model, and therefore allow the CRS model to be used. The total atmospheric Pb-210 inventory (DPM/cm²), required in the CRS model calculation, has been chosen (96.750 DPM/cm²) such that the CRS model predicted exactly the same average soil accumulation rate (0.5262 g/cm²/yr) as the linear regression model through the entire core length (0 - 38 cm). With the CRS model calibrated, it has been used to calculate ages for entire core.

The average soil accumulation rate, from core surface to the extrapolated bottom depth of any section, can be calculated by dividing the cumulative dry mass at the bottom of the extrapolated section by the calculated age at that depth. For example, the average soil accumulation rate, from the core surface to the bottom of section 12 (extrapolated depth 25cm) can be calculated as: $11.390 / 21.9 = 0.5201 \text{ g/cm}^2/\text{yr}$.

Conclusion:

The significant presence of Cs-137 throughout the core indicates that all sections are less than 53 years old (post 1963). Based upon the shape of Cs-137 profile, it is likely that the 1963 maximum atmospheric Cs-137 input could be recorded below 38 cm depth. The CRS model indicates an age of 32.7 yr at the bottom of the core (38 cm depth), an age compatible with the presence of Cs-137.

Over the entire core, the average soil accumulation rate estimated by the CRS model has been forced to exactly coincide with the linear regression estimate of 0.5262 g/cm²/yr. Although the CRS calculated ages depend upon the results of the linear regression model, the CRS model is to be preferred because it should provide accurate age predictions at the bottom of each section even though the soil accumulation rate is changing with time.

Overall, the analytical quality of radioisotope data (based upon the results of re-soil analyses and blanks) is considered good.

RESTORATION SITE >15 YEARS OLD: REITAN

INTERPRETATION

Observations:

Since the salinity was not measured in situ, it is estimated as 17.5 g/kg, the average of 10 g/kg and 25 g/kg (a range suggested by client). All Pb-210, Ra-226 and Cs-137 activities within this written report have been salt corrected.

Due to the presence of pebbles, each section was freeze dried, ground and then sieved through a 2-mm stainless steel mesh. The fine sample material which passed through the mesh (<2 mm) was subsampled for radioisotope analyses. It is assumed that pebbles >2mm do not contain detectable Pb-210, Ra-226 or Cs-137. Pebbles were not analyzed, but the masses were recorded and then used for the mass correction in the calculation of activities.

In this core, the Pb-210 activities are low, varying between 0.65 - 1.01 DPM/g below 4 cm depth, and gradually increase to 1.89 DPM/g in the surface section (depth 0 - 2 cm). The dry bulk densities are relatively high, ranging between 0.888 - 1.918 g/cm³.

Ra-226 was measured at 0.61, 0.59 and 0.78 DPM/g in sections 2 - 4 cm, 12 - 14 cm and 22 - 24 cm, respectively. The Pb-210 activity (1.05 DPM/g) seen in section 2 (2 - 4 cm) is significantly higher than the Ra-226 activity measured in the same section, indicating that detectable atmospheric sourced Pb-210 is present in the upper 4 cm. Below 4 cm, each measured Pb-210 activity barely exceed the nearest neighbouring Ra-226 measurement, indicating no presence of detectable atmospheric source Pb-210.

Cs-137 was measured in all 7 sections in the upper 14 cm of the core. Trace amount of Cs-137 was observed in sections 0 - 2 cm and 8 - 10 cm, and no detectable Cs-137 was found in the rest of the samples analyzed.

Regression model of Unsupported Pb-210 activity vs. Cumulative Dry Weight (g/cm²):

The regression model cannot be applied to this core, because only two samples near the core surface contain detectable unsupported Pb-210, based upon the Ra-226 measurements and the shape of Pb-210 profile.

CRS model of Age at bottom of Extrapolated section in years vs. Depth of bottom edge of current section in cm:

The CRS model cannot be applied to this core, because only two samples near the core surface contain detectable unsupported Pb-210, based upon the Ra-226 measurements and the shape of Pb-210 profile.

Conclusion:

In this core, detectable atmospheric sourced Pb-210 was observed only in the upper 4 cm (section 0 - 2 cm and section 2 - 4 cm). Below 4 cm depth, the soil was probably due to the placement of dredged material. Since the dredged material does not contain detectable atmospheric sourced Pb-210, it could possibly consist of soil older than 66 years (~ 3 half-lives of Pb-210).

If one assumes that 1) dredged material placement occurred 15 years ago, and 2) at 4 cm depth (lower depth of section 2 - 4 cm) it represents the surface of dredged material, i.e. natural accumulation of soil started at 4 cm, then the average soil accumulation rate at this sampling site can be estimated as: 4 cm / 15 years = 0.27 cm/yr, or 4.300 (g/cm²) / 15 years = 0.287 g/cm²/yr.

Overall, the analytical quality of radioisotope data (based upon the results of repeat analyses and blanks) is considered good.

REFERENCE SITE: CHRISTMAS BAY

INTERPRETATION

Observations:

The Pb-210 activity profile of this core shows an irregular, but approximately exponential decrease as a function of depth. The maximum activity of 4.37 DPM/g observed in the uppermost section (depth 0 - 2 cm) is about 7.5 times the lowest activity of 0.58 DPM/g in the bottom section (extrapolated depth 31 - 34 cm).

The dry bulk density in this core increases from 0.174 g/cm³ in the uppermost section to 0.681 g/cm³ in section 3 (depth 4 - 6 cm) and gradually decreases to 0.356 g/cm³ in section 6 (extrapolated depth 9 - 13 cm). Below 13 cm (extrapolated depth), the dry bulk density rapidly increases to 1.673 g/cm³ in section 13 (extrapolated depth 23 - 27 cm) and then varies between 1.483 - 1.673 g/cm³ in deeper sections.

Ra-226 was measured at 0.40 and 0.31 DPM/g in sections 10 - 12 cm and 32 - 34 cm respectively. Net unsupported Pb-210 was calculated by subtracting the nearest neighbouring Ra-226 measurement from each total Pb-210 value. The Pb-210 activity (0.58 DPM/g) seen in the bottom section (depth 32 - 34 cm) is significantly higher than the Ra-226 activity measured in the same section, indicating that the background level of Pb-210 has not been achieved in this core.

Cs-137 was measured in 15 sections throughout the entire core. Except four sections 0 - 2 cm, 20 - 22 cm, 22 - 24 cm and 32 - 34 cm, the Cs-137 activities were significantly above background, varying between 0.13 - 0.52 DPM/g.

Since the salinity was not measured in situ, it is estimated as 17.5 g/kg, the average of 10 g/kg and 25 g/kg (a range suggested by client). All Pb-210, Ra-226 and Cs-137 activities within this written report have been salt corrected.

Regression model of Unsupported Pb-210 activity vs. Cumulative Dry Weight (g/cm²):

When applying the linear regression model, it is assumed that the input of Pb-210 and the soil accumulation rate are constant. Although variation in the soil accumulation rate is apparent, the linear regression model was applied to sections 1 - 8 (depth 0 - 16 cm), because it appears that the average soil accumulation rate in this core interval will be reasonably estimated. This estimate of soil accumulation rate is used to calibrate the CRS model.

The regression model predicts ($R^2 = 0.7259$) an average soil accumulation rate of 0.1827 g/cm²/yr when a Pb-210 background of 0.3995 DPM/g (closest to the Ra-226 activity of 0.40 DPM/g measured in the 10 - 12 cm section) is chosen from the regression table. The age at the bottom of any core section can be estimated by dividing the cumulative dry weight/cm² by the accumulation rate. For example, the age at the bottom of section 4 (extrapolated depth 9 cm) is calculated as $4.100 / 0.1827 = 22.4$ yr.

CRS model of Age at bottom of Extrapolated section in years vs. Depth of bottom edge of current section in cm:

The CRS model assumes constant input of Pb-210 and a core that is long enough to include all of the measurable atmospheric source Pb-210, i.e. it contains a complete Pb-210 inventory. Since the second assumption is not satisfied in this core (background has not been achieved), it is not normally possible to apply the CRS model. However, in this core it is possible to calibrate the CRS model against the linear regression model, and therefore allow the CRS model to be used. The total atmospheric Pb-210 inventory (DPM/cm²), required in the CRS model calculation, has been chosen (22.895 DPM/cm²) such that the CRS model predicted exactly the same average soil accumulation rate (0.1827 g/cm²/yr) as the linear regression model in core interval of 0 - 16 cm. With the CRS model calibrated, it has been used to calculate ages for the upper 16 cm of the core.

The average soil accumulation rate, from core surface to the extrapolated bottom depth of any section, can be calculated by dividing the cumulative dry mass at the bottom of the extrapolated section by the calculated age at that depth. For example, the average soil accumulation rate, from the core surface to the bottom of section 4 (extrapolated depth 9 cm) can be calculated as: $4.100 / 18.8 = 0.2181 \text{ g/cm}^2/\text{yr}$.

Data below 16 cm of the core were excluded from CRS model due to suspicious rapid increase in dry bulk density profile.

Conclusion:

It appears that in the upper 16 cm the soil accumulated regularly at this sampling site. The significant presence of Cs-137 observed in core interval of 2 - 20 cm indicates that the soil accumulated above 20 cm depth are probably less than 53 years old (post 1963). The CRS model indicates an age of 45.2 yr at the bottom of section 8 (16 cm depth), an age compatible with the presence of Cs-137.

Over the core interval of 0 - 16 cm, the average soil accumulation rate estimated by the CRS model has been forced to exactly coincide with the linear regression estimate of 0.1827 g/cm²/yr. Although the CRS calculated ages depend upon the results of the linear regression model, the CRS model is to be preferred because it should provide accurate age predictions at the bottom of each section even though the soil accumulation rate is changing with time.

Overall, the analytical quality of radioisotope data (based upon the results of repeat analyses and blanks) is considered good.

Alternative interpretation:

In the upper 13 cm (extrapolated depth), the samples contain plenty of vegetation, while the samples below 16 cm contain more clay without any vegetation. The dry bulk density also increased significantly below 16 cm of the core. These observations suggest that the soil below 16 cm depth was probably due to the dredged material placement.

Section 8 (extrapolated depth 13 - 16 cm) appears to be a mix of dredge material and regularly accumulated soil. If one assumes that 1) dredged material placement occurred 15 years ago, and 2) at 14.5 cm depth (midpoint depth of section 13 - 16 cm) it represents the surface of dredged material, i.e. natural accumulation of soil started at 14.5 cm, then the average soil accumulation rate at this sampling site can be estimated as: $14.5 \text{ cm} / 15 \text{ years} = 0.97 \text{ cm/yr}$, or $7.343 \text{ (g/cm}^2) / 15 \text{ years} = 0.49 \text{ g/cm}^2/\text{yr}$.

These estimates are about 3 times higher than the CRS model results. The discrepancy may be due to a potential sediment slump event (sections 4 - 6 cm and 6 - 8 cm). This disturbance in the sediment accumulation process increases the uncertainty in modeling results.